Optimization of RAE Satellite Boom Deployment Timing

EDGAR J. BOWERS JR.* AND CHARLES E. WILLIAMS†
Applied Physics Laboratory, Johns Hopkins University, Silver Spring, Md.

The dynamics of deploying long extendible booms from the Radio Astronomy Explorer (RAE) satellite are analyzed to determine a method of deployment which will result in gravity gradient capture when the booms are completely extended. A phase-plane technique is used to determine approximate sensitivity to various parameters. It is shown that predeployment attitude and antenna Vee-angle are critical, whereas predeployment attitude rate and deployment rate are less important. An iterative program for correctly timing the two stages of deployment for various system parameters is developed. Also, a method of determining acceptable initial conditions for deployment is developed. These methods are combined in a real-time computer program to determine optimum start time, and optimum schedules for a two-stage deployment. Several results from the RAE-A boom deployment are included.

Introduction

THIS paper describes the boom deployment dynamics of the Radio Astronomy Explorer (RAE) satellite and the development of a computer program to optimally time this boom deployment.

The RAE satellite antennas (Fig. 1) are four tubular booms, 750 ft in length, which receive radio signals from intergalactic space, and also provide gravity gradient torque to control satellite attitude. In addition, two 320-ft damper booms are used to damp vehicle attitude librations and boom flexing. These six booms are initially stored in the satellite central hub, and after launch are reeled out to their desired length. It is desirable that when the booms are fully extended the satellite will be as nearly vertical as possible in order to achieve gravity-gradient capture. Thus, the basic problem is to time deployment of the booms in order to achieve the desired length and to simultaneously minimize resulting librations about local vertical.

J. L. Vanderslice[1] describes a method of first deploying one pair of booms from a satellite, and then another pair to achieve gravity stabilization. This concept was modified for the RAE, resulting in deployment of all four booms simultaneously in two separate phases. RAE deployment sequences to 750 ft are considered in Refs. 2 and 3 with the emphasis on flexing.

This paper concentrates on two major areas 1) determining optimum start time of main boom deployment and damper deployment, and 2) determining the optimum schedule for main boom deployment, which must be accomplished in at least two phases. In addition, we attempt to provide insight into the general problem of controlling a satellite by deploying booms. Finally, numerical results obtained during the actual RAE deployment on July 22, 1968 are presented. (The main booms were deployed to 450 ft, and the damper booms to 270 ft.)

Mathematical Analysis

To describe the RAE satellite attitude dynamics, the spacecraft is characterized by the following model. A rigid central hub is the reference platform from which attitude is measured. The four main booms are deployed from the hub in the XZ plane at angles of 30°, −30°, 150°, and −150° with the local vertical as shown in Fig. 1. The damper booms are rigidly connected together, and are deployed in the XY plane at an angle of 65° from the X axis. Boom bending is not considered in this paper, since a separate analysis revealed that at lengths up to about 450 ft boom bending does not significantly affect vehicle attitude dynamics.

To generate the vehicle attitude history, equations of motion are derived, using the Lagrange method. The significant steps in this procedure are as follows.

1) Define the generalized coordinates. Since the damper boom is locked during deployment, three generalized coordinates are sufficient to describe the attitude dynamics. Three Euler angles (ϕ = roll, θ = pitch, and ψ = yaw) are used to determine the angular orientation of the vehicle relative to a right-handed local coordinate frame defined by $(+Y_L)$ along the orbit pole and $(+Z_L)$ along the upward local vertical, as displayed in Fig. 1; this local frame rotates with respect to inertial space by the orbital rate vector having $\mathbf{X}_L$, $\mathbf{Y}_L$, and $\mathbf{Z}_L$ components $(0,\omega_0,0)$, respectively. The transformation matrix $[C]$, relating the satellite reference axes to the local axes is defined as

$$[C] = [\theta]_y[\phi]_x[\psi]_z \tag{1}$$

where $[X_i]_v$ denotes an orthogonal matrix defining a positive rotation of X_i radians about the v axis.

2) Specify the system's kinetic energy. The kinetic energy for this model is[4]

$$T = \tfrac{1}{2}\boldsymbol{\omega}^T[I]\boldsymbol{\omega} = \tfrac{1}{2}(\dot{\mathbf{X}} - \boldsymbol{\omega}_0)^T[M]^T[I][M](\dot{\mathbf{X}} - \boldsymbol{\omega}_0) \tag{2}$$

where $\boldsymbol{\omega}$ is the inertial angular rate vector of the satellite expressed in vehicle coordinates, $[I]$ is the satellite inertia matrix, $\dot{\mathbf{X}} = (\dot{\phi},\dot{\theta},\dot{\psi})^T$, and

$$[M] \triangleq \begin{bmatrix} \cos\psi & -\cos\phi\sin\psi & 0 \\ \sin\psi & \cos\phi\cos\psi & 0 \\ 0 & \sin\phi & 1 \end{bmatrix} \tag{3}$$

is the kinematical transformation matrix relating $\boldsymbol{\omega}$ and $\dot{\mathbf{X}}$.

3) Specify the system's potential energy. The gravitational potential energy of this system is[4]

$$V = \tfrac{3}{2}(\mu/R^3)\boldsymbol{\zeta}^T[I]\boldsymbol{\zeta} \tag{4}$$

where R is the magnitude of the satellite radius vector, $\boldsymbol{\zeta} = [C]^T\mathbf{1}_3$ is the unit vertical vector expressed in satellite coordinates, and μ is the Earth's gravitational constant. (In general, $\mathbf{1}_i$ = is a 3-vector whose i component is one, and the other 2 are zero).

Received August 13, 1969; presented as Paper 69-920 at the AIAA/AAS Astrodynamics Conference, Princeton, N.J., August 20–22, 1969; revision received December 17, 1969. This work was done for Goddard Space Flight Center under Contract NAS9753-20 (RAE).

* Senior Engineer, Systems Engineering.
† Associate Staff Engineer, Attitude Control.

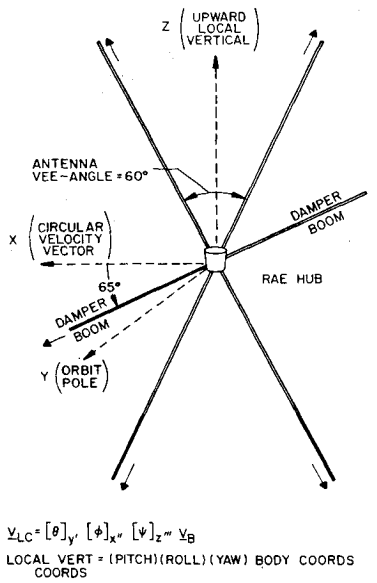

Fig. 1 RAE geometry and sign conventions.

4) Formulate the system's Lagrangian. The Lagrangian, denoted as L, for this system is

$$L = T - V = \tfrac{1}{2}\{(\dot{\mathbf{X}} - \boldsymbol{\omega}_0)^T[M]^T[I][M] \times (\dot{\mathbf{X}} - \boldsymbol{\omega}_0) - (3\mu/R^3)\boldsymbol{\zeta}^T[I]\boldsymbol{\zeta}\} \quad (5)$$

5) Generate the dynamic equations from the Lagrangian. The Lagrange equations of motion are

$$d(\partial L/\partial \dot{X}_i)/dt - \partial L/\partial X_i = 0 \quad (i = 1,2,3) \quad (6)$$

For this formulation, $\dot{X}_i = \dot{\phi},\dot{\theta},\dot{\psi}$ and $X_i = \phi,\theta,\psi$ for i = 1, 2, 3, respectively. Performing the indicated operations on the Lagrangian, a set of three nonlinear, second-order differential equations are obtained. These are

$$[K](\ddot{\mathbf{X}} - \dot{\boldsymbol{\omega}}_0) + [\dot{K}](\dot{\mathbf{X}} - \boldsymbol{\omega}_0) - \mathbf{N} + (3\mu/R^3)\mathbf{S} = 0 \quad (7)$$

where

$$[K] = [M]^T[I][M] \quad (8)$$

$$[\dot{K}] = (d/dt)[K] \quad (9)$$

$$\mathbf{N} = \{(\dot{\mathbf{X}} - \boldsymbol{\omega}_0)^T[M]^T[I][M_1](\dot{\mathbf{X}} - \boldsymbol{\omega}_0);\ 0 \quad (\dot{\mathbf{X}} - \boldsymbol{\omega}_0)^T[M]^T[I][M_3](\dot{\mathbf{X}} - \boldsymbol{\omega}_0)\}^T \quad (10)$$

$$[M_j] = (\partial/\partial X_j)[M] \quad (11)$$

$$\mathbf{S} = \{\boldsymbol{\zeta}^T[I]\boldsymbol{\zeta}_1;\ \boldsymbol{\zeta}^T[I]\boldsymbol{\zeta}_2;\ \boldsymbol{\zeta}^T[I]\boldsymbol{\zeta}_3\}^T \quad (12)$$

$$\boldsymbol{\zeta}_j = (\partial/\partial X_j)\boldsymbol{\zeta} \quad (13)$$

The effects of boom deployment are accounted for by a time-varying inertia matrix. This is included in the matrix, $[\dot{K}]$, i.e.,

$$[\dot{K}] = \{d[M]^T/dt\}[I][M] + [M]^T\{d[I]/dt\}[M] + [M]^T[I]\{d[M]/dt\} \quad (14)$$

For periods when the booms are not deploying, the second term in Eq. (14) is zero.

Equations (7–14) are the matrix equations used to describe the vehicle attitude dynamics. Numerical solution of these equations requires subsidiary equations to generate the time-dependent vehicle inertia matrix $[I]$, and the orbit parameters R, ω_0, and $\dot{\omega}_0$. The inertia matrix is determined by

$$[I] = [I_h] + \frac{1}{3}\sum_{j=1}^{6}(\rho_j L_j^3\{E_{33} - \mathbf{U}_j\mathbf{U}_j^T\}) \quad (15)$$

where ρ_j is the j boom linear density, $\mathbf{U}_j$ is the 3-vector of direction cosines (in vehicle coordinates) of the j boom, E_{33} is the 3×3 identity matrix and $[I_h]$ is the inertia of the central hub, which is insignificant for any appreciable boom lengths. When the booms are deploying, the changing inertia rate is

$$[\dot{I}] = \sum_{j=1}^{6} L_j^2\dot{L}_j(E_{33} - U_jU_j^T)\rho_j \quad (16)$$

where $\dot{L}_j$ is the j boom rate. The time-varying orbit parameters R, ω_0, and $\dot{\omega}_0$ are generated using Kepler's orbit equations for the restricted two-body model.

Equations (1–16) form the basis of a computer program used to simulate behavior of the RAE satellite, and for real-time operational support during the RAE-A flight. The computer program uses a modified Hamiltonian function, ΔH, as a deployment criterion. This function is now derived. The Hamiltonian has the following general definition[5]:

$$H = \left\{\sum_{i=1}^{3}\dot{X}_i\left(\frac{\partial L}{\partial \dot{X}_i}\right)\right\} - L \quad (17)$$

where L is the system's Lagrangian. Substituting Eq. (5) for L in Eq. (17) yields the specific expression for H for this system

$$H = \tfrac{1}{2}\{\dot{\mathbf{X}}^T[M]^T[I][M]\dot{\mathbf{X}} - (\omega_0^2)\mathbf{1}_2^T[M]^T[I][M]\mathbf{1}_2 + (3\mu/R^3)\boldsymbol{\zeta}^T[I]\boldsymbol{\zeta}\} \quad (18)$$

H is a function of the Euler angles and rates as well as the orbit parameters and the vehicle inertia configuration. The key to the usefulness of the Hamiltonian is that for a circular orbit and an unchanging vehicle inertia matrix H is constant. This is true in general when the Lagrangian is not an explicit function of time.

H could be used directly to evaluate the attitude dynamics after a deployment, but it is desirable to use a function which is semi-positive-definite and vanishes when all state

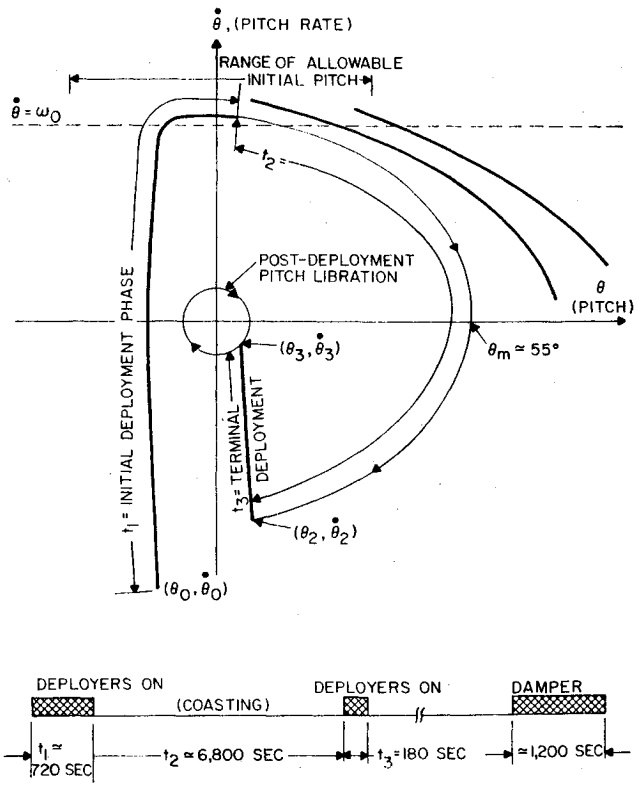

Fig. 2 Typical pitch phase-plane trajectory for main boom deployment.

variables are zero. This can be done by subtracting from H the value of the Hamiltonian when all state components (angles and rates) are zero. Thus

$$\Delta H = H - H_0 = H - \tfrac{1}{2}\omega_0^2\{-\mathbf{1}_2{}^T[I]\mathbf{1}_2\} - (3\mu/2R^3)\mathbf{1}_3{}^T[I]\mathbf{1}_3 \quad (19)$$

The function ΔH is a positive-definite function of all the state variables and is used (Sec. 5) as a measure of vehicle libration energy.

Pitch-Plane Analysis

Preliminary analysis showed that the four RAE main booms must be deployed in at least two phases, separated by a period of half an orbit. A typical "deadbeat" deployment sequence for main boom deployment to 450 ft is illustrated at the bottom of Fig. 2. The booms are deployed out to 360 ft (at 0.5 fps), then the deployers are turned off for $t_2 \simeq 6800$ sec. The remaining length of 90 ft is unreeled during the second deployment phase. Note that this phase occurs prior to damper deployment.

Some insight into the main boom deployment process can be obtained by limiting satellite motion to the pitch plane, a valid approximation for small roll and yaw. It is emphasized that the following analysis [Eqs. (20–27)] is approximate and the operational program used Eqs. (1–19) as equations of motion. For small roll and yaw, Eq. (7) reduces to the following equation for pitch, a well-known result[6]

$$\ddot{\theta} = -3\omega_0^2 \sin\theta \cos\theta \left(\frac{I_x - I_z}{I_y}\right) + \frac{\dot{I}_y}{I_y}(\omega_0 - \dot{\theta}) \quad (20)$$

The typical pitch phase plane at the top of Fig. 2 can be generated by solving Eq. (20) for the deployment sequence shown. When the deployers are turned on (at θ_0, $\dot{\theta}_0$ in Fig. 2), the rapidly increasing inertia of the satellite virtually stops the rotational motion with respect to inertial space. This corresponds to a pitch rate equal to orbital rate, since the local vertical is rotating at orbital rate in inertial space. Thus, the initial deployment phase results in a phase-plane trajectory which is a nearly vertical ascent to the line $\dot{\theta} = \omega_0$. During this period, acceleration is almost entirely due to the term $(\dot{I}_y/I_y)(\omega_0 - \dot{\theta})$ in Eq. (20). However, when $\dot{\theta}$ approaches ω_0, the pitch rate becomes nearly constant, so that the phase-plane trajectory follows the line $\dot{\theta} = \omega_0$.

We found that good approximations to the results at the end of the first deployment phase are as follows:

$$\theta_1 \simeq \theta_0 + \omega_0 t_1 \qquad \dot{\theta}_1 \cong \omega_0 \quad (21)$$

These equations indicate that the initial pitch rate has little effect on results, and that the coasting phase will always be initiated from some point near the line $\dot{\theta} = \omega_0$, with the location of this point dependent upon the initial pitch θ_0 and the time t_1.

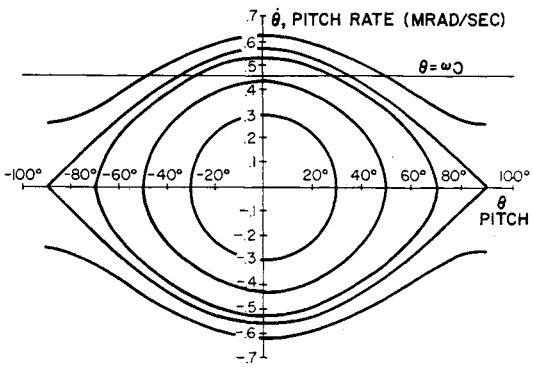

Fig. 3 Family of coasting trajectories for nominal RAE geometry.

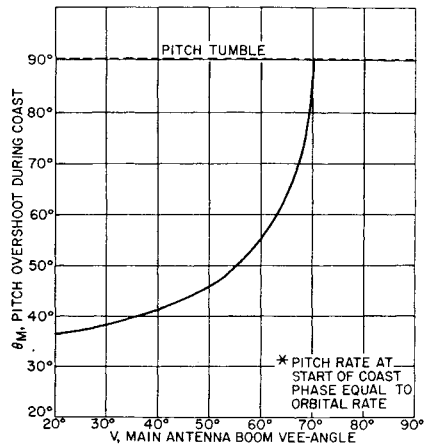

Fig. 4 Pitch overshoot during coast period as function of antenna Vee-angle.

During the coasting phase, $\dot{I}_y = 0$ and Eq. (20) can be reduced to

$$\dot{\theta}^2 = 2k(\sin^2\theta_{\max} - \sin^2\theta) \quad (22)$$

where $k = 1.5\omega_0^2(I_x - I_z)/I_y$ and $\theta_{\max}$ is the maximum pitch during the coasting period. A plot of Eq. (22) in the phase-plane yields ellipse-like figures intersecting the θ axis at $\pm\theta_{\max}$ and the $\dot{\theta}$ axis at $\dot{\theta}_{\max} = (2k)^{1/2}\sin\theta_{\max}$. A family of coasting trajectories for a given value of k is illustrated in Fig. 3. The figures are nearly circular near the origin if the scales are chosen properly and become more elongated with increasing $\dot{\theta}_{\max}$, until $\dot{\theta}_{\max} > 1/(2k)^{1/2}$ for which $\sin\theta_{\max} > 1$. This corresponds to an unstable situation in which the vehicle is tumbling about the pitch axis. In order to have a successful deployment, this situation must be avoided, i.e., $(\dot{\theta}^2/2k + \sin^2\theta) < 1$ is required in order to stay on one of the closed trajectories.

Equation (22) can also be used to show the dependence of the maximum pitch overshoot $\theta_{\max}$ on the antenna Vee-angle V. For $\theta_1 = 0$, $\dot{\theta}_1 = \pm\dot{\theta}_{\max}$, and

$$\sin\theta_{\max} = \theta_{\max}/(2k)^{1/2} = \dot{\theta}_{\max}/\omega_0(3\cos V)^{1/2} \quad (23)$$

If the effective Vee-angle of the antennas is increased (due to a bent boom), it is obvious that $\theta_{\max}$ will be increased. Equation (23) is plotted in Fig. 4 for $\dot{\theta}_{\max} = \omega_0$, a reasonable value. Evidently, the upper limit on the Vee-angle allowing a successful deadbeat deployment is 70°.

The corridor of acceptable coasting trajectories for deployment is bounded by two constraints: 1) $\dot{\theta}_{\max}$ must be at least large enough for the coasting trajectory to intersect the line $\dot{\theta} = \omega_0$ in order to be an achievable condition at the end of the first deployment phase, and 2) $\dot{\theta}_{\max}$ must be small enough so that the pitch overshoot angle $\theta_{\max}$ is within allowable limits.

The correct coasting time t_2 required to arrive at the $(\theta,\dot{\theta})$ origin with $L = 450$ ft also depends strongly on the initial pitch angle at deployment initiation. Figure 5 shows how coasting time varies with initial pitch, for deployment to 450 ft. It is possible to start at pitch angles ranging from about $-30°$ to $+20°$.

The terminal deployment phase will now be considered. The deploying booms again drive the phase plane trajectory toward $\dot{\theta} = \omega_0$ but deployment termination occurs (ideally) at the origin. During this phase, the gravity gradient term in Eq. (20) is small relative to the deployment torque, and the equation is approximated by

$$\ddot{\theta} = (\dot{I}_y/I_y)(\omega_0 - \dot{\theta}) \quad (24$$

$$\dot{I}_y/I_y = 4\rho L^2\dot{L}/(I_{hy} + 4\rho L^3/3) \simeq 4\rho L^2\dot{L}/4\rho L^3/3 \quad (25)$$

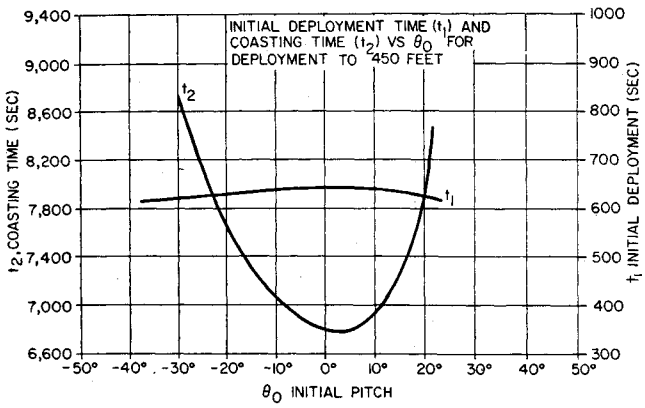

Fig. 5 Initial deployment time and coasting time for deployment to 450 ft.

where ρ is the linear mass density of the boom and I_{hy} is the hub inertia. If the deployment rate L is constant, then

$$\dot{I}_y/I_y \cong 3\dot{L}/L = 3/(\text{total deployment time}) \quad (26)$$

This simple relationship is significant, for it explains the somewhat unexpected result that deployment rate has little effect on satellite dynamics, the important parameter being the total time during which the booms have been deployed. In other words, if the booms were deployed at 0.4 fps instead of 0.5 fps and the nominal deployment schedule adhered to, the satellite dynamics would be virtually unaffected. (Of course, final boom length would be shorter.) This effect has been verified numerically by computer simulation.

The principal conclusions drawn from the pitch plane analysis are that initial pitch and antenna Vee-angle have a strong effect on main boom deployment dynamics, whereas initial pitch rate and deployment rate do not. In addition, it was found that deployment can be initiated from a wide range of initial values ($-20°$ to $+30°$) of pitch.

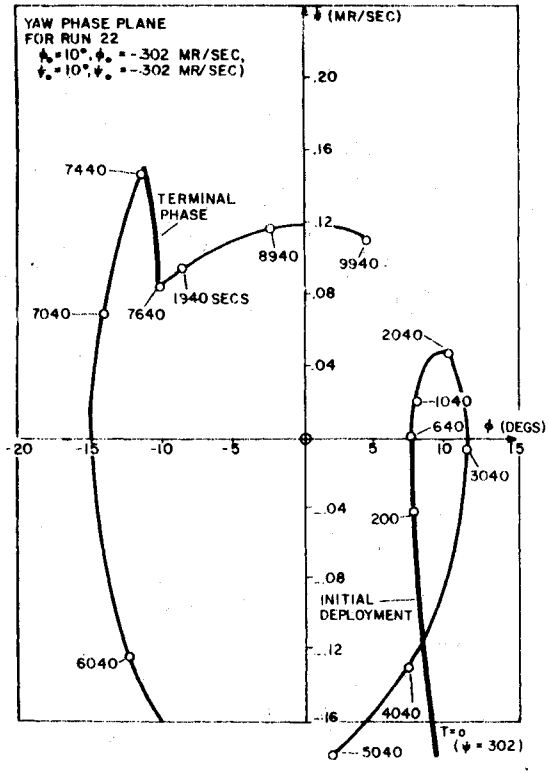

Fig. 6 Yaw phase plane for deadbeat deployment sequence.

Pitch Optimization Logic

The pitch plane analysis of the previous section is useful in obtaining approximate results. However, generation of a deployment sequence for a real situation requires the use of a more complete physical model, including orbital eccentricity and complete three-dimensional dynamic equations. The deployment problem is now stated as follows: define a deployment sequence to reduce roll, pitch, and yaw and their corresponding rates $(\phi,\theta,\psi,\dot{\phi},\dot{\theta},\dot{\psi})$ to zero at some desired boom length. This problem cannot be solved in general with a deadbeat deployment sequence, since only two independent control variables, t_1 and t_2, are available to control six parameters. Thus, a compromise is called for, but one which will leave the satellite as close to a local vertical orientation as possible at the end of deployment.

Applying the phase-plane analysis to roll and yaw dynamics revealed that these angles are not as easily controlled by main boom deployment as pitch. This is shown by comparing the pitch phase-plane plot with similar plots for roll and yaw in Figs. 6 and 7. The general strategy, as before, is to wait until the angle has nearly reached zero, and then deploy the booms until the phase-plane trajectory is driven through the coordinate origin. However, comparison of Figs. 2, 6, and 7 reveals that this cannot be done because the pitch, roll, and yaw do not approach zero at the same time. In addition, controlling roll and yaw presents the problem that the desired final rate is zero inertial rate, rather than orbital rate, as in the case of pitch. The difficulty in achieving this can be appreciated by realizing that the angle rates before and after terminal deployment are approximately

$$\left(\frac{\dot{\phi}_3}{\phi_2}\right) \cong \left(\frac{I_{x2}}{I_{x3}}\right), \left(\frac{\dot{\theta}_3 - \omega_0}{\dot{\theta}_2 - \omega_0}\right) \cong \left(\frac{I_{y2}}{I_{y3}}\right)\left(\frac{\dot{\psi}_3}{\dot{\psi}_2}\right) \simeq \left(\frac{I_{z2}}{I_{z3}}\right) \quad (27)$$

To achieve the desired final values of $\dot{\phi}_3 = 0$ and $\dot{\psi}_3 = 0$, it is evident that infinite inertia changes are required, whereas to achieve the desired value of $\dot{\theta}_3 = 0$, the ratio of initial and final inertias is $\omega_0/(\dot{\theta}_2 - \omega_0) \simeq 0.5$. The aforementioned analysis is not exact, of course, but is given as a heuristic explanation of the difficulty in tailoring a deployment sequence to eliminate roll and yaw libration.

Since librations about all three axes cannot be reduced with a deadbeat deployment, and since control of yaw and roll appears to be difficult, the deployment timing is tailored to reduce the pitch librations and accept the yaw and roll librations that result. A simple method of determining t_1 and t_2 is obtained numerically using the equations of motion listed in Sec. 2, and a pitch optimization logic, which is now discussed.

In Fig. 2, the use of an arbitrary deployment schedule results in completion of deployment at $(\theta_3,\dot{\theta}_3)$, which results in a libration circle of radius θ_L. It is desired to modify the times t_1, t_2, and t_3 to arrive at the coordinate origin rather than $(\theta_3,\dot{\theta}_3)$. Since the terminal deployment trajectory is nearly vertical, $\dot{\theta}_3$ can be reduced to zero by adjusting t_3. The desired change in the terminal leg δt_3 can be determined from the final pitch rate by

$$\delta t_3 = -\dot{\theta}_3/\ddot{\theta}_3 \quad (28)$$

θ_3 can be reduced to zero by adjusting the coasting time t_2. It was found that the shape of the terminal trajectory was essentially independent of θ_2. Thus, a change in pitch prior to terminal deployment results in a like change in pitch after deployment, i.e.,

$$\delta\theta_2 \simeq \delta\theta_3 \quad (29)$$

Also, since the coasting trajectory is nearly horizontal at $(\theta_2,\dot{\theta}_2)$, changes in θ_2 are directly proportional to δt_2. From these relationships, the method of adjusting t_2 to eliminate θ_3 is apparent, i.e.:

$$\delta t_2 = \theta_3/\dot{\theta}_2 \quad (30)$$

Equations (29) and (30) form the basis for the pitch optimization logic used in the computer program. This logic consists of choosing some approximate schedule (t_1,t_2,t_3), running the computer program through this deployment sequence, and using the terminal values of pitch and pitch rate thus obtained to determine a modified schedule (t_1',t_2', t_3') for the succeeding run, i.e.,

$$t_1' = t_1 - \delta t_3,\ t_2' = t_2 + \delta t_2,\ t_3' = t_3 + \delta t_3 \qquad (31)$$

Note that the initial deployment time is reduced by δt_3 in order to deploy the desired boom length L_D, i.e., ($t_1 + t_3$) is held constant.

The pitch optimization logic is an iterative process so that the computer program reruns each new schedule until θ_3 and $\dot{\theta}_3$ are virtually zero. The process converges quickly for a wide range of initial conditions, usually giving good results on the first iteration.

Some typical computer runs illustrating convergence are summarized in Table 1. The runs include a nominal case, with all initial angles and rates zero, and other cases with deviations as indicated. The pitch optimization logic gave good results on the first iteration of every case, even in the worst case, where the orbital eccentricity of 0.1 resulted in a terminal pitch angle of $\theta = 21°$ on the first try. The pitch optimization logic also gave a reduction in ψ_{max}, which is a measure of total libration energy (including roll and yaw) discussed in the next section.

Hamiltonian Analysis

The pitch optimization logic is used to determine an optimum deadbeat deployment sequence, given some nominal starting time and attendant initial conditions. However, the deployment problem also requires determination of whether or not the chosen initial time-point is optimum, that is, in the case of continually changing dynamics, it may be more desirable to start a deployment action at one time than at another. In particular, it is possible to limit the final roll and yaw librations by optimum selection of start time.

The principal problem is determining a meaningful optimization criterion to use in evaluating the success of a particular damper deployment. This problem is difficult because the various attitude state components (angles and angle rates) are strongly coupled. Thus, direct examination of the state just after damper deployment does not necessarily reveal what the state will be at some later time. In particular, the RAE-A inertia ratios are such that the vehicle is less tightly stabilized in yaw than in either pitch or roll. Numerical results from computer runs have verified that the vehicle may undergo a large excursion in yaw, or even a yaw flip ($\psi > 90°$), if enough energy couples into the yaw dynamics. Thus, a reasonable parameter for evaluating damper deployment is the maximum predicted yaw angle.

Table 1 Computer results evaluating pitch optimization law convergence[a]

Case	Try	θ_3, degs	$\dot{\theta}_3$, deg/sec	δt_2, secs	δt_3, secs	ψ_{max}, degs
Nominal	1	−4.41	$-0.79(10^{-3})$	−164	8	13.97
	2	0.10	$-0.10(10^{-3})$	4	1	1.20
	3	0.00	$0.00(10^{-3})$	0	0	0.07
$\theta_0 = -10°$	1	2.40	$-0.73(10^{-3})$	92	8	5.95
	2	0.21	$0.21(10^{-3})$	8	−2	2.15
	3	−0.06	$0.00(10^{-3})$	−2	0	1.71
$\phi_0 = 10°$, $\psi_0 = -30°$	1	−11.28	$1.07(10^{-3})$	−480	−12	>90
	2	−0.26	$-0.35(10^{-3})$	−11	4	58.3
	3	0.06	$0.01(10^{-3})$	2	−1	57.1
eccentricity = 1	1	−21.07	$-2.13(10^{-3})$	−807	24	>90
	2	0.75	$-1.15(10^{-3})$	27	15	14.9
	3	0.11	$0.31(10^{-3})$	4	−4	12.8

[a] Note: δt_2 = indicated change in coasting time. δt_3 = indicated change in terminal deployment time. θ_3 = pitch angle at deployment termination. $\dot{\theta}_3$ = pitch rate at deployment termination. ψ_{max} = upper bound of post-deployment yaw libration, based on Hamiltonian ΔH.

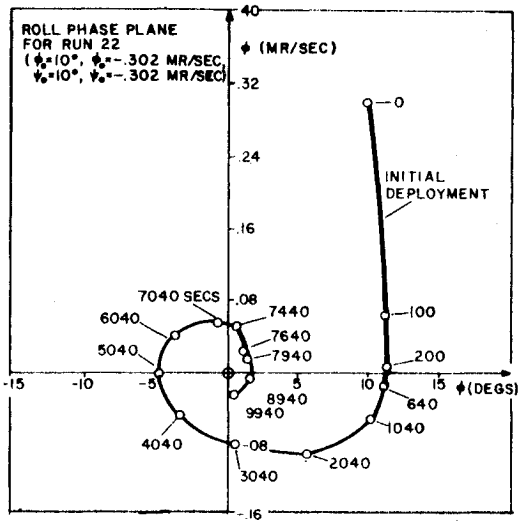

Fig. 7 Roll phase plane for deadbeat deployment sequence.

The modified Hamiltonian function ΔH defined by Eq. (19) has been used to predict maximum yaw angle in order to compare the results of one deployment sequence with another. The properties of ΔH which make it useful for this purpose are a) ΔH is constant in time (for a circular orbit); b) ΔH is a function of all the state variables, i.e., roll, pitch, yaw, and the three attitude rates; c) ΔH is a positive-definite function of the state variables, i.e., $\Delta H = 0$ when the three angles and rates are zero.

Setting two of the angles and all three rates to zero, the following expressions are derived from Eq. (19):

$$\varphi_{max} = \sin^{-1}\{[\Delta H/2\omega_0^2(I_y - I_x)]^{1/2}\} \qquad (32)$$

$$\theta_{max} = \sin^{-1}\{[\Delta H/3\omega_0^2(I_x - I_z)]^{1/2}\} \qquad (33)$$

$$\psi_{max} = \sin^{-1}\{[2\Delta H/\omega_0^2(I_y - I_x)]^{1/2}\} \qquad (34)$$

The inertia ratios of the RAE satellite are such that ψ_{max} is always considerably larger than ϕ_{max},θ_{max} after either main boom deployment, or the subsequent damper deployment. Thus, ΔH is used to determine the maximum yaw angle (ψ_{max}) which can result from a particular deployment.

Using Eqs. (31 and 32–34) to determine the maximum value of the roll, pitch, and yaw angles, the natural questions

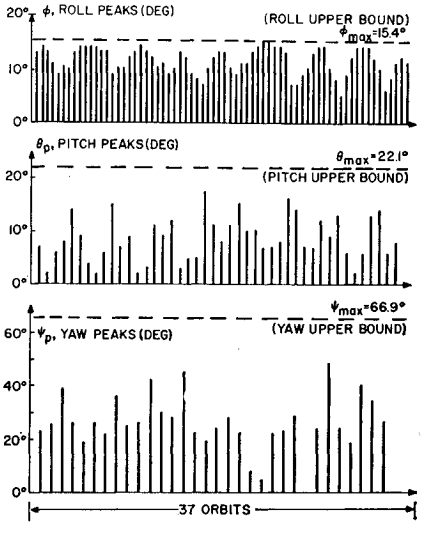

Fig. 8 Comparison of angle peaks after main boom deployment with upper bounds determined from ΔH.

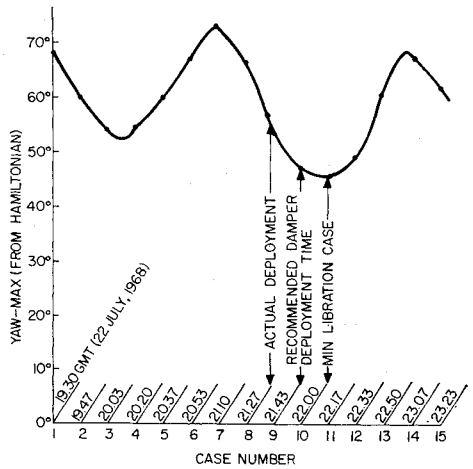

Fig. 9 Numerical results from damper deployment to 270 ft on RAE-A mission.

arise. Are these equations unduly pessimistic? Can most of the energy ever get into yaw (or roll or pitch) so that the calculated maximum angle is closely approached? An analytical proof is not yet available, but numerical results show that the computed values of ϕ_{max},θ_{max}, ψ_{max} are realistic estimates of the maximum angle excursions which will occur within a reasonable time.

A computer run employing the equations of motion described in Sec. 2 was made to determine how closely the computed values of ϕ_{max}, θ_{max}, and ψ_{max} are approached. The case run was one in which initial roll and yaw angles of $\phi_0 = -20°$ and $\psi_0 = 20°$ resulted in the occurrence of substantial librations after termination of main boom deployment. The modified Hamiltonian ΔH was evaluated at two time points: just after completion of main boom deployment and 37 orbits later. The ΔH was identical for the two points, and predicted upper bounds on each angle were $\phi_{max} = 15.4°$, $\theta_{max} = 22.1°$, and $\psi_{max} = 66.9°$.

Because of the length of the computer run, the complete time history plot cannot be included here, but a summary of the positive peaks of each angle is shown in Fig. 8. The results differ, depending on the angle considered. The roll time history is a fairly regular, nearly sinusoidal curve of radian frequency twice the orbit rate, as expected. Roll peaks average about 13°, as compared to the predicted maximum of 15.4°.

Pitch and yaw time histories exhibit a less regular pattern. The predicted maximum yaw angle is 66.9°, whereas the largest positive yaw peak is 48°. If a yaw peak ψ_p accounts for 70% of the modified Hamiltonian ΔH, then $\psi_p = \sin^{-1}\{0.7 \sin (66.9)\} = 40°$. Figure 8 shows that ψ_p exceeds 40° four times in the 37 orbits. Counting negative peaks, the expected occurrence of yaw peaks greater than 40°, or less than −40°, is eight times in 37 orbits, or about once per 4 or 5 orbits.

Analysis of the pitch peaks yields similar results. $\theta_p = \sin^{-1}\{0.7[\sin(22.1)]\} = 15°$. Figure 8 shows four positive peaks of 15° or greater, corresponding to eight occurrences in 37 orbits of pitch angles greater than 15° or less than −15°.

The previous results are for the configuration after main boom deployment. Another 37-orbit run was made for the configuration after damper deployment, but with the damper still locked. The results again showed that the attitude angles are sensibly bounded by ϕ_{max}, θ_{max}, and ψ_{max}. The over-all conclusion of the preceding analyses is that $\psi_{max} < 90°$ is a somewhat conservative, but realistic criterion to apply to satellite dynamics after boom deployment.

Op-1 Computer Program

The Op-1 program utilizes the equations of motion derived in Sec. 2 as well as the pitch optimization logic and Hamiltonian just described. The purpose of the program was twofold: to generate parametric analyses of acceptable deployment sequences, and to provide real-time support on the RAE-A flight.

The nominal mission profile illustrates two uses of the program. Mode 1 is the timing of first main boom deployment, and mode 4 the timing of damper deployment. Both modes utilize the Hamiltonian as a deployment criterion and, in addition, mode 1 utilizes the pitch optimization logic to time the two main boom phases.

Assume that at some time t_0, it is desired to determine an optimum deployment time in the interval $t_1 - t_n$. The program integrates equations of motion to update the state $(\mathbf{X},\dot{\mathbf{X}})t_0$ to various trial deployment times t_1, $t_2 - t_n$ in the interval. Deployment is simulated starting from each of these times and ψ_{max} is computed from the postdeployment state for each of the trials, as shown by Eqs. (33) and (19). The lowest value of ψ_{max} indicates the optimum deployment time. If the proposed deployment is for main booms, the pitch optimization logic is employed at each trial start time; damper deployment evaluation does not require this.

The RAE-A satellite was launched on July 4, 1968. On July 22, the main booms were deployed to 450 ft, and the damper booms were deployed to 270 ft. Some of the results obtained using mode 4 to predict the optimum damper deployment timing are illustrated in Fig. 9. The individual points shown are the ψ_{max} results (employing the Hamiltonian) for damper deployment at each of the times indicated. A total of 15 cases, spanning an orbit, were computed at about 19.00 GMT. All cases showed ψ_{max} well below 90°, indicating that damper deployment was reasonable at any time during the orbit, with an optimum deployment at about 22.17 GMT. Precise optimization was not vital during the actual flight, due to the small librations after main boom deployment and deployment was initiated by RAE-A control personnel at 21.44 GMT to ensure complete coverage by the Ororal tracking station in case the damper deployment rate was slower than expected.

References

[1] Vanderslice, J. L., "Appendix to Memo BBD-1354," July 10, 1964, Johns Hopkins Applied Physics Lab., Silver Spring, Md.

[2] Dow, P. C. et al., "Interim Report for Investigation of the Dynamic Characteristics of a V Antenna for the RAE Satellite," RAD TR-65-28, Sept., 1965, Avco Corp., Wilmington, Mass.; also CR-962, NASA.

[3] Dow, P. C. et al., "Dynamic Stability of a Gravity Gradient Stabilized Satellite Having Long Flexible Antennas," *AIAA/JACC Guidance and Control Conference*, AIAA, New York, 1966.

[4] Newton, J. K. and Farrell, J. L., "Natural Frequencies of a Flexible Gravity-Gradient Satellite" *Journal of Spacecraft and Rockets*, Vol. 5, No. 5, May 1968, pp. 560–569.

[5] Goldstein, H., "Conservation Theorems and Symmetry Properties," *Classical Mechanics*, Addison-Wesley, Reading, Mass., 1955, pp. 53–54.

[6] Liu, H. S. and Mitchell, J. P., "The Structural and Librational Dynamics of a Satellite Deploying Flexible Booms or Antennas," AIAA Paper 67-43, New York, 1967.